Nonlinear quantum light generation in collective spontaneous emission supplementary material

Offek Tziperman[1†], Gefen Baranes[2†], Alexey Gorlach[1†*], Ron Ruimy[1], Chen Mechel[1], Michael Faran[4], Nir Gutman[1], Andrea Pizzi[3] and Ido Kaminer[1*]

[1]Technion – Israel Institute of Technology, Haifa 32000, Israel
[2]Massachusetts Institute of Technology, Cambridge, Massachusetts 02139, USA
[3]Harvard University, Cambridge, Massachusetts 02138, USA
[4]Tel Aviv University, Ramat Aviv 69978, Israel

[†]equal contributors, [*]kaminer@technion.ac.il, [*]horlach@campus.technion.ac.il

Table of Contents

I. Light inside a cavity

I.1 Density matrices and Wigner functions of the emitters and cavity light

The master equation for emitters and cavity light reads [1]–[4]:

$$\dot{\rho}_{\mathrm{in}}(t) = \mathrm{i}[\rho_{\mathrm{in}}(t), H_{\mathrm{in}}] + \mathcal{D}[\rho_{\mathrm{in}}(t)], \tag{S1}$$

where the Hamiltonian is $H_{\mathrm{in}} = H_{\mathrm{E}} + H_{\mathrm{EC}} + H_{\mathrm{C}}$ and the dissipator is $\mathcal{D}[\rho_{\mathrm{in}}(t)] = \kappa c \rho_{\mathrm{in}}(t) c^{\dagger} - \frac{1}{2}\kappa\{c^{\dagger}c, \rho_{\mathrm{in}}(t)\}$ and it accounts for leakage from the cavity at rate κ. In Eq. (S1), $H_{\mathrm{E}} = \Omega_0 \sum_{i=1}^{N} \sigma_i^z = \Omega_0 S^z$ is the Hamiltonian of the emitters, which are considered as two-level systems with transition frequency Ω_0. The term $H_{\mathrm{EC}} = (g c^{\dagger} S^{-} + g^{*} c S^{+})$ describes the interaction between the emitters and the cavity mode, assuming that the emitters couple to the field with the same coupling coefficients. The annihilation and creation operators are $c, c^{\dagger}$, and $S^{\pm} = \sum_{i=1}^{N} \sigma_i^{\pm}$ are the collective raising and lowering operators, with $\sigma_i^{\pm} = \sigma_i^x \pm i\sigma_i^y$. The term $H_{\mathrm{C}} = \Omega_1 c^{\dagger} c$ is the Hamiltonian of the cavity field. We consider $\Omega_1 = \Omega_0$ below.

We solve Eq. (S1) numerically. For N indistinguishable emitters, the density matrix ρ_{in} is a tensor product of two $(N+1) \times (N+1)$ matrices at the initial time, one for the single-mode cavity field and one for the emitters. The density matrix of the emitters is found by tracing out the cavity field:

$$\rho_{\mathrm{emitters}}(t) = \mathrm{Tr}_{\mathrm{light\,in}}\big(\rho_{\mathrm{in}}(t)\big). \tag{S2}$$

The Wigner function $W_{\mathrm{emitters}}(\theta, \phi)$ of the emitters on the Bloch sphere yields [5]:

$$\begin{cases} W_{\mathrm{emitters}}(t, \theta, \phi) = \sum_{k=0}^{N} \sum_{q=-k}^{k} \rho_{kq}(t) Y_{kq}(\theta, \phi) \\ \rho_{kq}(t) = \sum_{m=-N/2}^{N/2} \sum_{m'=-N/2}^{N/2} (-1)^{N/2-m} \sqrt{2k+1} \begin{pmatrix} N/2 & k & N/2 \\ -m & q & m' \end{pmatrix} \langle m' | \rho_{\mathrm{emitters}}(t) | m \rangle \end{cases}, \tag{S3}$$

where $\begin{pmatrix} N/2 & k & N/2 \\ -m & q & m' \end{pmatrix}$ are 3j symbols and $|m\rangle$ are the permutationally symmetric state of the emitters corresponding to $m + N/2$ excited emitters.

On the other hand, the density matrix of the cavity light is found by tracing out the emitters:

$$\rho_{\mathrm{light\,in}}(t) = \mathrm{Tr}_{\mathrm{emitters}}\big(\rho_{\mathrm{in}}(t)\big). \tag{S4}$$

The Wigner function of the light inside the cavity $W_{\mathrm{light\,in}}(t, X, P)$ yields [6], [7]:

$$W_{\mathrm{light\,in}}(t, X, P) = \frac{1}{\pi} \int_{-\infty}^{+\infty} \langle X - y | \rho_{\mathrm{light}}(t) | X + y \rangle e^{-2iPy} dy\,. \tag{S5}$$

I.2 The dynamics of the light inside the cavity

In the main text, we focus on the light emitted outside the cavity. Here, we also analyze the dynamics of the cavity field itself. For a *reabsorption efficiency* ξ of order unity, the light inside the cavity will have no quantum features, in the sense of a positive Wigner function at all times, as shown in Figure 2 in the main text. The loss of light to the modes outside the cavity causes decoherence of the fragile quantum state inside the cavity, which becomes an incoherent mixture. More interesting is the case of a strong reabsorption efficiency $\xi \gg 1$ instead, when the Rabi frequency in the cavity is much larger than the decay rate from it. In such a case, coherent oscillations occur between the cavity field and the emitters. We consider a fully inverted initial condition (all emitters excited), as can be obtained from a π-pulse excitation. The resulting Wigner functions of the cavity light and emitters are shown in Fig. S1b. We also obtain the intensity of light inside the cavity

$$I_{\text{inside}}(t) = \hbar\Omega_1 \frac{d}{dt}\langle c^\dagger c\rangle, \tag{S6}$$

plotted in Fig. S1c, and the negativity [8] of the combined cavity-emitters density matrix $\rho_{\text{in}}(t)$, shown in Fig. S1d. The negativity is a measure of the degree of entanglement between the emitters and the light, according to the PPT criterion for separability [9], which is defined by:

$$\text{negativity} = \frac{|\rho^{\Gamma_A}|_1 - 1}{2}, \tag{S7}$$

with ρ^{Γ_A} the partial transpose with respect to the emitters and $|\cdot|_1$ the L_1 norm.

In Fig. S1 we show the coherent transfer of energy back and forth between the emitters and the cavity. The zeros of the intensity in Fig. S1c, e.g., at times t_0, t_2, t_4 correspond to the times at which the energy is absorbed by emitters, or the energy is completely transferred to the light. Indeed, at these times, the negativity is at its minimal value as shown in Fig. S1d. The cavity's Wigner function has negative parts at some times, see e.g., Fig. S1a at time t_2. Furthermore, we observe a state transfer between the emitters and the cavity field and the fidelity of the state transfer increases as the reabsorption efficiency ξ increases. When the emitters and the cavity field are strongly entangled (large negativity), e.g., at time t_1, the cavity Wigner function is completely positive, because tracing out the emitters leads to an incoherent mixture

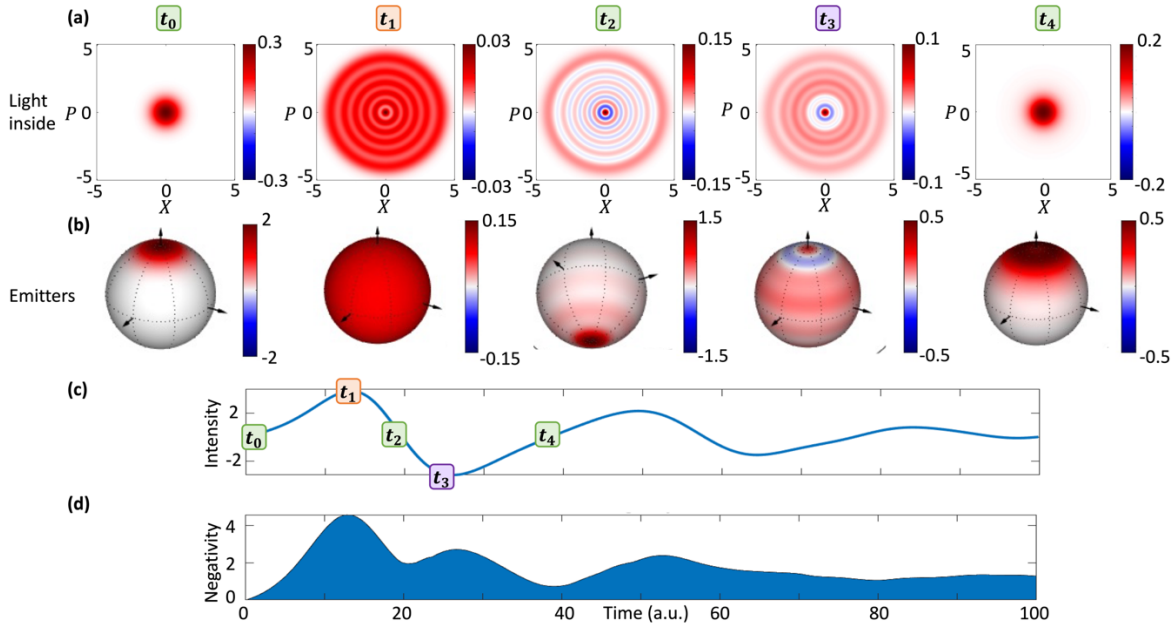

Fig S1. Cavity field and emitters' dynamics. (a) Wigner function of the cavity field at selected times $t_0 = 0, t_2 = 19.7, t_4 = 38.3$ (zero intensity), $t_1 = 13.2$ (first intensity maximum), and $t_3 = 26.1$ (first intensity minimum). **(b)** Emitters' Wigner function, at the same selected times. **(c)** Intensity of the cavity field as function of time. **(d)** The negativity of ρ_{in} which shows the entanglement between light and the emitters. The parameters used in the simulation are: $\xi = 2Ng^2/\kappa^2 = 2.25 \cdot 10^3$, and $N = 10$ emitters.

The dynamics shown in Fig. S1 is characteristic for large reabsorption efficiencies $\xi = 2g^2N/\kappa^2$, that is, for a regime when the cavity losses are small compared to the Rabi frequency. Away from this limit, in Fig. S2 we compute the maximum (over time) of the negative area of Wigner function, namely $V = \max_t \int_{(x,p):W_{\text{light in}}<0} (-1) W_{\text{light in}}(t,x,p) dxdp$. We find that the Wigner function of the light in cavity is everywhere positive if $\xi \leq \xi_c$, while it has negative parts for $\xi > \xi_c$, for some critical reabsorption efficiency ξ_c. We note that ξ_c depends on the number of emitters and on the initial conditions.

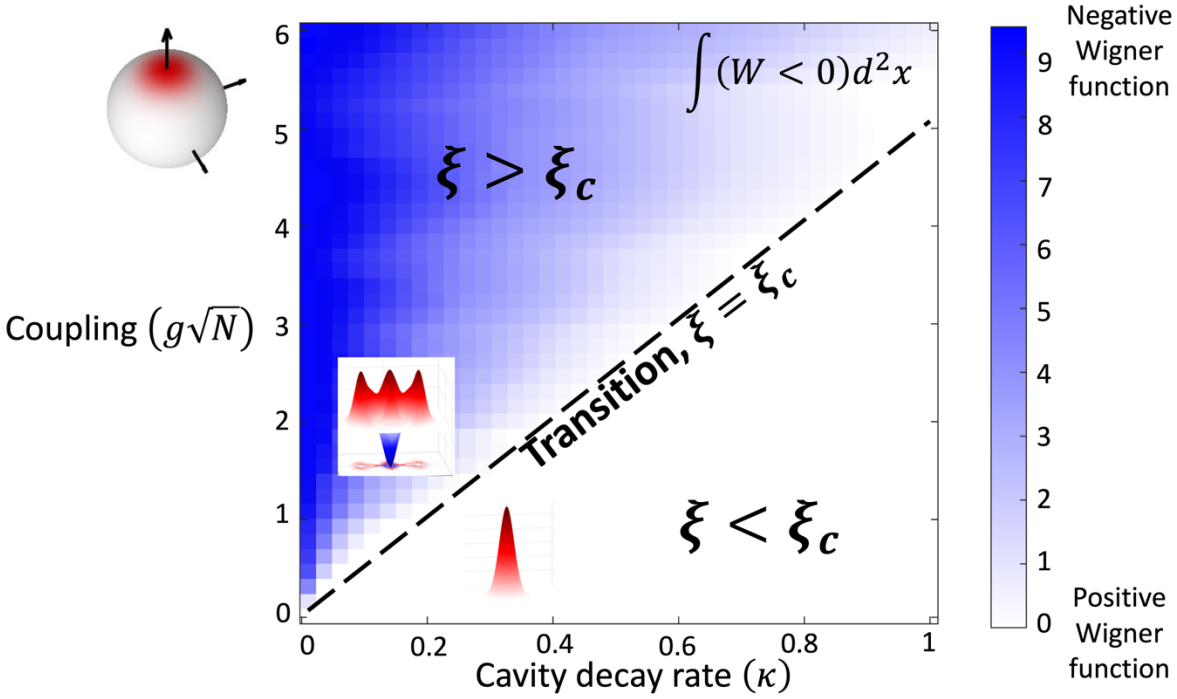

Fig. S2. Regimes of superradiant emission in a cavity. Wigner function maximum negative area for different interaction strengths ($g\sqrt{N}$) and photon losses (κ). The Wigner function can have negative parts if $\xi > \xi_c$, thus the losses outside the cavity are small. The emitters are initially excited, as plotted on the Bloch sphere on the left. Two cavity Wigner functions are plotted as insets representing the $\xi > \xi_c$ and $\xi < \xi_c$ regimes. The number of emitters is $N = 10$.

II. Pulses of quantum light

II.1 Modes

The electromagnetic field can be quantized in different bases [10]. By far the most common is the plane wave mode basis, which in one dimension takes the form $a_\omega, a_\omega^\dagger$ with $\left[a_\omega, a_{\omega'}^\dagger\right] = \delta(\omega - \omega')$. Another example is the basis of time given by the Fourier transform $a(t) = \frac{1}{\sqrt{2\pi}} \int_{-\infty}^{\infty} a_\omega e^{i\omega t} d\omega$. In many cases, these bases are not optimal, and it is more efficient to quantize the field in a wavepacket basis. Furthermore, sometimes it is not possible to describe the emission as a single mode. For example, if a single emitter is excited twice, emitting two single-photon wave packets at different times, the quantum state of light is fundamentally a two mode state.

If a state can be described as a single mode, then it is possible to define $a_0 = \int_{-\infty}^{\infty} \eta_0^*(t') a(t') dt'$, and then describe the state as a superposition:

$$\left|\psi_{\text{single-mode}}\right\rangle = \sum_n A_n \frac{\left(a_0^\dagger\right)^n}{\sqrt{n!}}|0\rangle. \tag{S8}$$

More generally, one can define a set of complex basis functions $\eta_n(t)$, orthonormal functions, and then define a general state with the set of operators $a_n = \int_{-\infty}^{\infty} \eta_n^*(t')a(t')dt'$. In the following analysis, we find the conditions for which the light emitted will be close to a single mode state, meaning that exists a single mode state to which it has high fidelity. In this case we find

$$\rho_0 = \text{Trace}_{n\neq 0}\{\rho\}, \tag{S9}$$

where ρ_0 is the quantum state of light in the highest occupied principal mode. We can find ρ_0 in two steps:

1. Finding the principal modes, and specifically the most occupied ones.
2. Finding the quantum state in these modes.

II.2 Emission modes

We define the *principal modes* as a minimal set of modes that contain all the quantum state information. Specifically, a set of orthonormal complex functions $\eta_n(t)$ defined via the annihilation operators $a_n = \int_{-\infty}^{\infty} \eta_n^*(t')a(t')dt'$. The *principal modes* satisfy for all $n > p$, $a_n\rho = 0$, and so also $\langle a_m^\dagger a_n\rangle = 0$, for all m. One can notice that the integer p is nothing but the rank of the $\Gamma^{(1)}(t_1, t_2)$ matrix:

$$\Gamma^{(1)}(t_1, t_2) = \left\langle a^\dagger(t_1)a(t_2)\right\rangle, \tag{S10}$$

which is Hermitian and thus diagonalizable. A possible set of principal modes can be found as the eigenvectors. Numerical diagonalization of $\Gamma^{(1)}(t_1, t_2)$ yields:

$$\Gamma^{(1)}(t_1, t_2) = \sum_i n_i \eta_i^*(t_1)\eta_i(t_2)\,, \tag{S11}$$

where n_i are the numbers of photons in each mode.

II.3 Quantum state of the most occupied mode

To derive a master equation to describe the most occupied traveling mode of light, we follow Kiilerich and Molmer [11], [12]. The key insight in their derivation is that a single mode state (as defined in II.1) can be absorbed perfectly into a fictitious one-sided cavity with a time-dependent coupling $g_0(t)$, the calculation of this coupling is repeated in Section II.4 for the

readers' convenience. A one-sided cavity with such coupling will at $t \to \infty$ acquire the state of the mode $\eta_0(t)$.

The problem can now be reduced to the coupling of a system operator O^- with:

$$a_{\mathrm{out}}(t) = a_{\mathrm{in}}(t) + O^-(t) \tag{S12}$$

to the fictitious cavity in a single master equation. To do this one must couple the output from the system into the fictitious cavity, but not couple the output from the fictitious cavity back into the system. The cascaded master equation reads for a single decay channel O^- and a single output mode [11]:

$$\dot{\rho} = i[\rho, H_{\mathrm{S}} + H_{\mathrm{I}}] + \sum_i (L_i \rho L_i^\dagger - \frac{1}{2}\{L_i^\dagger L_i, \rho\}). \tag{S13}$$

The part of the Hamiltonian describing the coupling between the mode and the fictitious cavity, $H_{\mathrm{I}} = \frac{i}{2}\left(g_0^* O^+ a_0 - g_0 O^- a_0^\dagger\right)$, transfers photons from the virtual cavity to the system and vice versa. To enforce unidirectionality, one must add a corresponding damping term $L_0 = O^- + g_0^*(t) a_0$, so that, for $O^- = \sqrt{\kappa c}$ and $H_{\mathrm{S}} = H_{\mathrm{E}} + H_{\mathrm{EC}} + H_{\mathrm{C}}$ as in Section I.1, Eq. (S13) matches Eq. (4) of the main text. We solve Eq. (4) numerically using the $\eta_0(t)$ corresponding to the most occupied mode, obtained as explained in the previous section, and obtain the density matrix ρ (of the combined system of emitters, cavity, and dominant leaking mode). The density matrix of the outgoing light in the dominant mode η is obtained as

$$\rho_0 = \mathrm{Tr}_{\mathrm{in}}(\rho), \tag{S14}$$

where $\mathrm{Tr}_{\mathrm{in}}(\dots)$ denotes trace over cavity field and emitters.

II.4 Coupling of the virtual cavity

As mentioned above, the dominant mode can be absorbed in a cavity through a suitable time-dependent coupling. To find this, consider the Heisenberg-Langevin equation for a_0 [13]:

$$\dot{a}_0 = -\frac{|g_0(t)|^2}{2} a_0 - g_0(t) b_{\mathrm{in}}(t), \tag{S15}$$

where $g_0(t)$ is the time-dependent coupling to the cavity. We can rewrite (S15) as:

$$\frac{d}{dt}\left(a_0 e^{\frac{1}{2}\int_0^t dt' |g_0(t')|^2}\right) = -g_0(t) b_{\mathrm{in}}(t) e^{\frac{1}{2}\int_0^t dt'' |g_0(t'')|^2}, \tag{S16}$$

integration on both sides yields:

$$a_0(t)e^{\frac{1}{2}\int_0^t dt'|g_0(t')|^2} - a_0(0) = -\int_0^t dt'\, g_0(t')b_{\text{in}}(t')e^{\frac{1}{2}\int_0^{t'} dt''|g_0(t'')|^2}, \tag{S17}$$

$$a_0(t) = a_0(0)e^{-\frac{1}{2}\int_0^t dt'|g_0(t')|^2} - \int_0^t dt'\, g_0(t')b_{\text{in}}(t')e^{-\frac{1}{2}\int_{t'}^t dt''|g_0(t'')|^2}. \tag{S18}$$

For the output mode $a_0(t)$ to aquire the mode of the shape $\eta_0(t)$, at the infinite time we should have:

$$a_0 = \int_0^\infty dt'\, \eta_0^*(t')b_{\text{in}}(t'). \tag{S19}$$

Comparing (S18) and (S19) yields:

$$-g_0(t)e^{-\frac{1}{2}\int_t^\infty dt''|g_0(t'')|^2} = \eta_0^*(t), \tag{S20}$$

from which:

$$\int_0^t dt'\, |g_0(t')|^2 e^{-\int_{t'}^\infty dt''|g_0(t'')|^2} = \int_0^t dt'\, |\eta_0(t)|^2, \tag{S21}$$

$$e^{-\int_t^\infty dt'|g_0(t')|^2} = \int_0^t dt'\, |\eta_0(t)|^2. \tag{S22}$$

Substituting (S22) in (S20), we get:

$$g_0(t) = -\frac{\eta_0^*(t)}{\sqrt{\int_0^t dt'\, |\eta_0(t')|^2}}. \tag{S23}$$

Notice that the denominator is exactly the square root of the fraction of the wave packet already absorbed in the cavity at time t.

III. Cavity QED Coupled to a Continuum of Modes

We first give more details on how to implement the calculation of $\Gamma^{(1)}(t_1, t_2)$, which is explained in the main text. The calculation of this matrix consists of two steps. The first involves relating the operators of light to the operators of the emitting system, as can be done with an input-output relation [14]. For example, in the case coupling the cavity mode to the continuum of frequency modes outside the cavity, the input-output relation will read: $a_{\text{out}}(t) = a_{\text{in}}(t) + \sqrt{\kappa}c(t)$, where the operators are given here in the Heisenberg picture. Assuming that the light outside the cavity is initially in the vacuum state, from the input-output relation we get:

$$\Gamma^{(1)}(t_1, t_2) = \langle a^\dagger(t_1)a(t_2)\rangle = \kappa\langle c^\dagger(t_1)c(t_2)\rangle. \tag{S24}$$

The right-hand side of Eq. (S24) can be calculated following standard procedures in quantum optics (quantum regression theorem) [15], [16]. Particularly, given $V(t,0)$ the nonunitary time evolution super operator combined cavity-emitters system, such that the density matrix is $\rho_{\text{in}}(t) = V(t,0)\rho_{\text{in}}(0)$, then:

$$\langle c^\dagger(t_1)c(t_2)\rangle = \text{Tr}\left(c^\dagger V(t_1,t_2)cV(t_2,0)\rho_{\text{in}}(0)\right). \tag{S25}$$

In other words, one must use the master equation Eq. (2) from the main text to evolve the initial density matrix $\rho_{\text{in}}(0)$ to a time t_2, multiply the result by the lowering operator c, evolve for a time $t_1 - t_2$, multiply times $c^\dagger$, and take the trace.

III.1 Modes of Dicke superradince in a cavity

Fig. S3 shows $\Gamma(t_1,t_2)$, the modes $\eta_i(t)$, and their occupations n_i. We consider both fully-inverted (a1,b1,c1) and cat state (a2,b2,c2) as initial conditions. The correlation function $\Gamma(t_1,t_2)$, in (a1,a2), features oscillations due to the coherent back-and-forth exchange of energy between emitters and cavity field. In the linear regime, when the number of excitations is much lower than the number of emitters, the emitting system can be approximated as a harmonic oscillator, and the dynamics are the same as light leaking out from a cavity. By this logic, the emitted light is mostly contained in a single mode. A fully inverted initial condition (a1) corresponds instead to a highly nonlinear regime. In this case, we still find almost 90% are within a single mode (c1), but a second and a third are non-negligible and contain more than 10% of the emission, leading to a lower purity of the emitted light, when tracing out these modes. For the atomic cat state (a2), the initial condition is lower on the Bloch sphere, thus further into the linear regime, leading to more predominant single-mode occupation (c2).

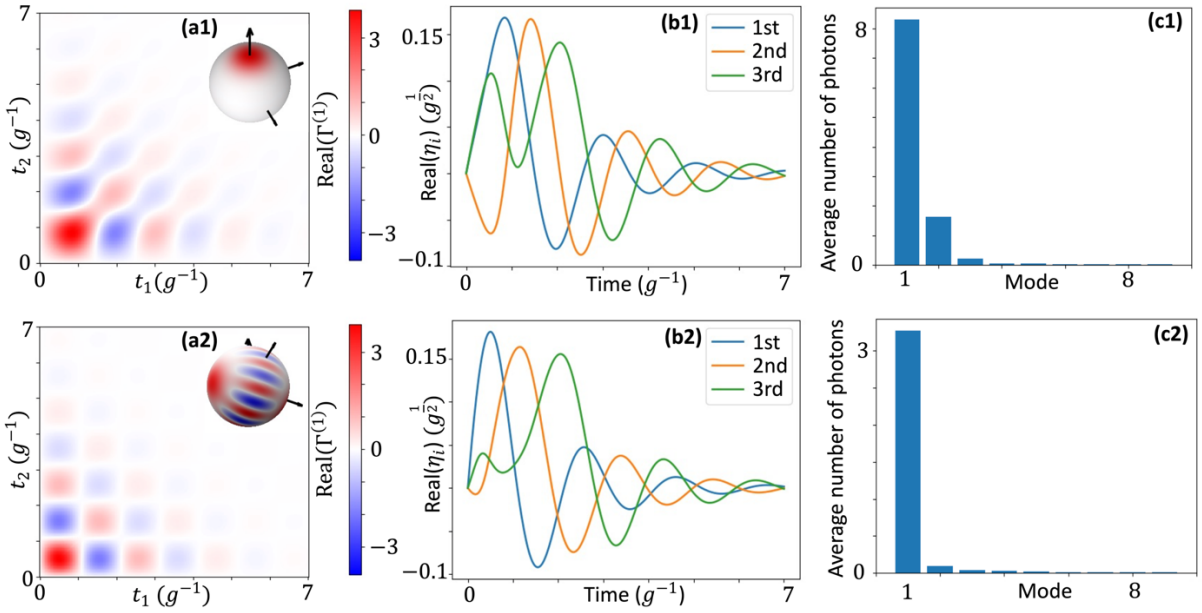

Fig. S3. Analysis of temporal modes outside the cavity. (a1,2) Normalized first-order coherence function for fully-inverted (1) and cat (2) state initial conditions. **(b1,2)** Real part of the first, second and third most occupied modes $\eta_i(t)$. **(c1,2)** Average number of photons of the 10 most occupied modes.

III.2 Intensity, spectrum, and entanglement entropy of the emitted light

The Wigner function of the light outside of the cavity is calculated similarly to the cavity field using Eq. (S5). The intensity plotted in Figure 2 in the main text is defined as:

$$I(t) = \langle a^\dagger a \rangle(t) = \kappa \langle c^\dagger c \rangle(t), \tag{S26}$$

Where the entanglement entropy plotted in Figure 2 is defined as:

$$\text{entanglement entropy} = -\text{Tr}(\rho_{\text{in}} \log_2(\rho_{\text{in}})), \tag{S27}$$

where $\rho_{\text{in}} = \text{Tr}_{\text{out}}(\rho)$ with $\text{Tr}_{\text{out}}(\dots)$ the trace over the light outside the cavity. We remark that the entire state of light all the temporal modes outside the cavity, light inside the cavity and emitters is pure such that the use of entanglement entropy is justified.

The spectrum is given by the Fourier transform of the coherence function $\Gamma(t_1, t_2)$, namely

$$S(\omega) = \langle a^\dagger(\omega) a(\omega) \rangle = \frac{1}{2\pi} \int_{-\infty}^{\infty} \int_{-\infty}^{\infty} \Gamma^{(1)}(t_1, t_2) e^{i\omega(t_2 - t_1)} \, dt_1 dt_2 \,, \tag{S28}$$

and is plotted in Fig. S4. We observe a transition between single to doubly peaked spectrums at a reabsorption efficiency $\xi \approx \frac{1}{2}$.

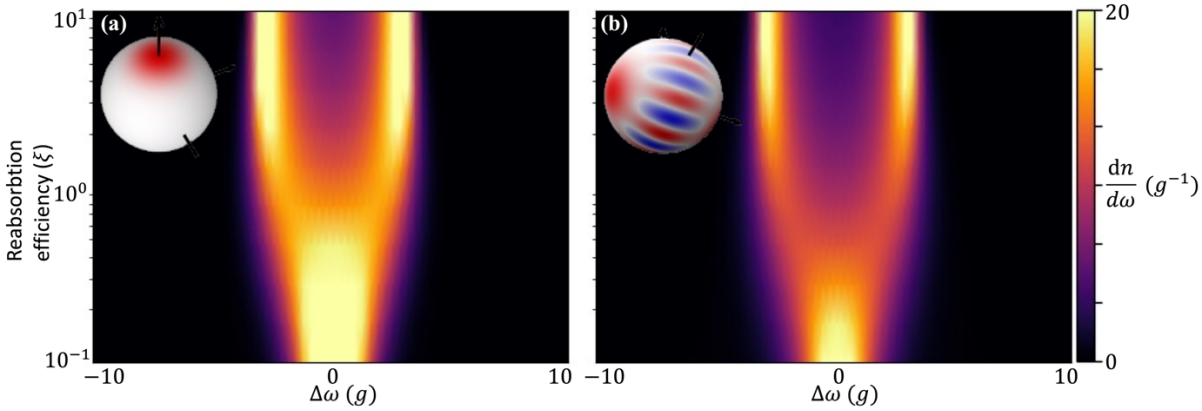

Fig. S4. Spectrum of the light emitted outside of the cavity. For low reabsorption efficiency, the spectrum of the emission is a single peak at zero frequency (in the rotating frame). For large reabsorption efficiencies, the back-and-forth energy transfer between the emitters and the cavity results instead in a finite-frequency double peak in the emission spectrum. The transition between these two scenarios happens at $\xi = \frac{1}{2}$. Here, we consider $N = 10$ emitters initially in the fully excited state (a) or cat state (b) as in Eq. (S77). The insets show the initial condition on the Bloch sphere.

IV. 1D Atomic Array Coupled to a Waveguide

This section summarizes how the theory can be applied to a one-dimensional atomic array coupled to a chiral waveguide. We consider emitters coupled to a waveguide at locations $\{z_n\}_{n=1}^N$. The Hamiltonian of the light-matter interaction reads:

$$H = H_{\mathrm{E}} + H_{\mathrm{EF}} + H_{\mathrm{F}}, \tag{S29}$$

$$H_{\mathrm{E}} = \Omega_0 \sum_{1\le n\le N} \sigma_n^{\mathrm{z}}, \tag{S30}$$

$$H_{\mathrm{EF}} = \sum_{1\le n\le N} \int_0^\infty dk g \sigma_n^+ a(k) e^{ikz_n} + \mathrm{h.c.}, \tag{S31}$$

$$H_{\mathrm{F}} = \int_0^\infty dk \omega(k) a^\dagger(k) a(k). \tag{S32}$$

where z_n is the location of the n-th emitter, $a(k)$ the annihilation operator of a mode with wavevector k along the waveguide axis, and g the coupling (assumed independent of the wavenumber and real for simplicity). We denote $\omega(k) = c|k|$ the frequency associated with the wavevector k, c being the speed of light in the medium.

IV.1 Input-output relation for waveguide QED

We repeat the derivation of the input-output relation for waveguide QED [17]. Heisenberg dynamics yields:

$$\dot{a}(k) = i[H, a(k)] = -i\omega(k)a(k) - ig \sum_{1\le n\le N} \sigma_n^- e^{-ikz_n}, \tag{S33}$$

from which:

$$\frac{d}{dt}\left(a(k)e^{i\omega(k)t}\right) = -ig \sum_{1\le n\le N} \sigma_n^- e^{-ikz_n} e^{i\omega(k)t}, \tag{S34}$$

which is solved by:

$$a(k,t) = a(k,0)e^{-i\omega(k)t} - ig\int_0^t dt' \sum_{1\le n\le N} \sigma_n^-(t')e^{-ikz_n} e^{i\omega(k)(t'-t)}. \tag{S35}$$

Fourier transforming $a(z,t) = 1/\sqrt{2\pi}\int_{-\infty}^{\infty} dk' a(k',t)e^{ik'z}$, from Eq. (S35) we get:

$$a(z,t) = \frac{1}{\sqrt{2\pi}}\int_{-\infty}^{\infty} dk a(k,0)e^{ik(z-ct)} - \frac{ig}{\sqrt{2\pi}}\int_{-\infty}^{\infty} dk \int_0^t dt' \sum_{1\le n\le N} \sigma_n^-(t')e^{-ik\left(c(t-t')+z_n-z\right)}. \tag{S36}$$

and so:

$$a(z,t) = a(z-ct,0) - \frac{i\sqrt{2\pi}g}{c}\int_0^t dt' \sum_{1\le n\le N} \delta\left(t - t' + \frac{z_n - z}{c}\right)\sigma_n^-(t'). \tag{S37}$$

The integral can be nonzero only if $z - z_n > 0$, and so:

$$a(z,t) = a\left(0, t - \frac{z}{c}\right) - i\sqrt{\frac{\Gamma_{1D}}{c}} \sum_{1\le n\le N} \theta(z - z_n)\sigma_n^-\left(t - \frac{z - z_n}{c}\right). \tag{S38}$$

with $\Gamma_{1D} = \frac{2\pi g^2}{c}$. Assuming that the typical timescale for the evolution of the system is much longer than the light crossing time, a Markov approximation yields $\sigma_n^-\left(t - \frac{z-z_n}{c}\right) \approx \sigma_n^-\left(t - \frac{z}{c}\right)e^{-\frac{i\Omega_0 z_n}{c}}$. We can define $a_{\text{out}}(t) = \sqrt{c}a(z_N^+, t)$, just to the right of the last emitter, and $a_{\text{in}}(t) = \sqrt{c}a\left(0, t - \frac{z}{c}\right)$:

$$a_{\text{out}}(t) = a_{\text{in}}(t) - i\sqrt{\Gamma_{1D}}S^-\left(t - \frac{z}{c}\right). \tag{S39}$$

with $S^-(t) = \sum_{1\le n\le N} \sigma_n^-(t)e^{-\frac{i\Omega_0 z_n}{c}}$. Eq. (S39) is the input-output relation we wanted.

IV.2 Principal modes and cascaded master equation for waveguide QED

Next, we follow a protocol like the one in the main text to find the $\Gamma^{(1)}(t_1, t_2)$ function and diagonalize it. This can be done with the input-output relation from Section (IV.1):

$$\Gamma^{(1)}(t_1, t_2) = \langle a^\dagger(t_1) a(t_2) \rangle = \Gamma_{1D} \langle S^+(t_1) S^-(t_2) \rangle. \tag{S40}$$

Let us now consider procedure from Section III.1 in more details. The input-output relation for 1D waveguide is described by Eq. (S39). The considered mode η_0 according to Eq. (S39) is described by:

$$a_0 = \int_0^t dt' \, \eta_0^*(t') a(t') = a_0 - i\sqrt{\Gamma_{1D}} \int_0^t dt' \, \eta_0^*(t') S^- \left(t' - \frac{z}{c}\right), \tag{S41}$$

we take the derivative with respect to time of this equation, and get:

$$\dot{a}_0 = -i\sqrt{\Gamma_{1D}} \eta_0^*(t) S^- \left(t - \frac{z}{c}\right), \tag{S42}$$

According to the proof in Section II.4 for $a_0(t \to \infty)$, the solution of Eq. (S42) is the same as:

$$\dot{a}_0 = -\frac{|g_0(t)|^2}{2} a_0 - i\sqrt{\Gamma_{1D}} g_0(t) S^- \left(t - \frac{z}{c}\right), \tag{S43}$$

where $g_0 = -\eta_0^*(t) / \sqrt{\int_0^t |\eta_0(t')|^2 dt'}$. The equation for S^- is described by the master equation

$$\dot{S}^-(t) = i[H_S, S^-(t)] + S^+(0) S^-(t) S^-(0) - \frac{1}{2}\{S^+(0) S^-(0), S^-(t)\}, \tag{S44}$$

The Eqs. (S43) and (S44) correspond to the master equation in Schrodinger picture:

$$\dot{\rho} = -i[H_S + H_I, \rho] + L_0 \rho L_0^\dagger - \frac{1}{2}\{L_0^\dagger L_0, \rho\}, \tag{S45}$$

with $H_S = \Omega_0 S_z - \frac{i\Gamma_{1D}}{2} \sum_{m,n} \left(\sigma_m^+ \sigma_n^- e^{\frac{i2\pi|z_m - z_n|}{\lambda_0}} - h.c. \right)$ describing the emitter energy levels and coherent interactions mediated by the waveguide, $H_I = \frac{i}{2}\sqrt{\Gamma_{1D}}(g_0^* S^+ a_0 - g_0 S^- a_0^\dagger)$, $L_0(t) = \sqrt{\Gamma_{1D}} S^- + g_0^*(t) a_0$, and $g_0 = -\eta_0^*(t) / \sqrt{\int_0^t |\eta_0(t')|^2 dt'}$. We can add terms $L_i \rho L_i^\dagger - \frac{1}{2}\{L_i^\dagger L_i, \rho\}$ to describe additional losses, with L_i for $i > 0$ being the jump operators for additional decay channels, such as spatial modes lost outside the waveguide.

To ensure a single decay channel, we considered in the main text a mirror at location $z_{\text{mirror}} = -\lambda_0/4$. The system Hamiltonian then becomes $H_S = \Omega_0 S_z - \frac{i\Gamma_{1D}}{4}\sum_{m,n}\left(\sigma_m^+\sigma_n^-\left(e^{\frac{i2\pi|z_m - z_n|}{\lambda_0}} + e^{\frac{i2\pi(z_m+z_n)}{\lambda_0}}\right) - h.c.\right)$, and the operators $S^{\pm} \equiv \sum_{1\le n\le N}\sigma_n^-(t)\cos\left(\frac{2\pi\Omega_0 z_n}{c}\right)$.

IV.3 Modes in waveguide QED

This section is devoted to studying the temporal modes of emission in waveguide QED, we consider emitters coupled to a non-chiral waveguide, with a single decay channel to only one side. This can be achieved by placing a mirror at $z_{\text{mirror}} = -m\lambda_0$ where m is a positive integer. In the case of $z_n = n\lambda_0$, the equations now take the form of a Dicke model allowing for a much simpler numerical solution. In Fig. S5 we solve for $z_n = n\lambda_0$, and an initial fully excited emitters state, and show the quantum state in the first two most occupied modes. The dynamics of the number of excited emitters (Fig. S5a) display the characteristic features of superradiance. The quantum state in the first mode is close to a Fock state with nine photons (Fig S5c), the number of initially excited emitters, while the second mode is almost unoccupied (Fig S5d).

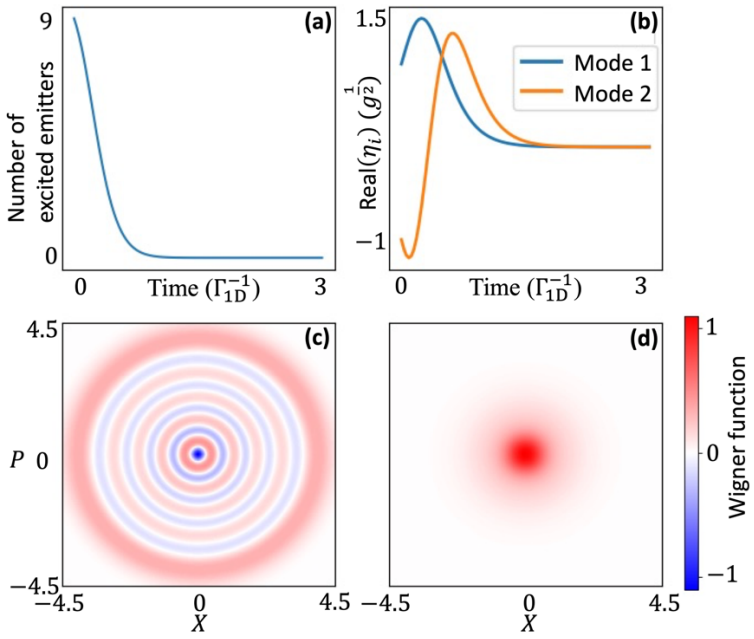

Fig. S5. Superradiance in waveguide QED. We consider the fully excited state of the emitters in the waveguide with spacing $z_n = n\lambda$. **(a)** The number of excited emitters versus time. **(b)** The two most occupied temporal modes. **(c)** The Wigner function of mode 1. **(d)** The Wigner function of mode 2. Here, we considered $N = 9$ emitters and no losses to other spatial modes.

Next, we study the modes of waveguide QED at different spacings, going beyond Dicke superradiance. Specifically, we consider $z_n = \frac{n\lambda}{2}$, and emitters initially in a coherent state obtained via a $\frac{7\pi}{12}$ excitation pulse from the axis perpendicular to the waveguide with a plane wave.

The emitters decay into a dark state, resulting in a nonzero number of excited emitters at the final time in Fig S6a. Light is emitted mostly into a single temporal mode, see Fig S6c, whose Wigner function features negative parts and is reminiscent of that of a cat state.

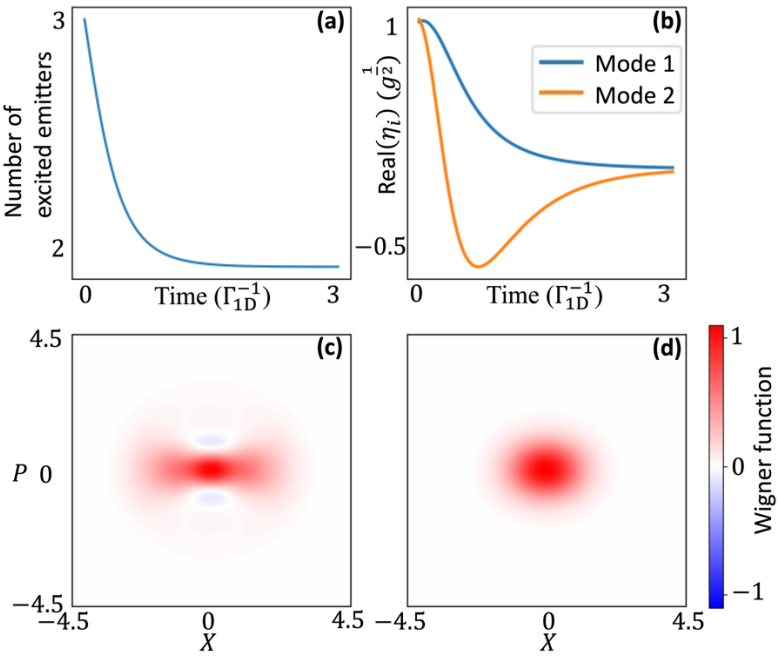

Fig. S6. Emission in waveguide QED far from the Dicke limit. We consider the emitters excited by a $7\pi/12$ pulse in a waveguide with spacing $z_n = n\lambda/2$. **(a)** Number of excited emitters versus time. The inversion population fails to decay to zero within the considered times, pointing to a dark state. **(b)** The two most occupied modes as a function of time. **(c)** The Wigner function in mode 1. Nonclassical features (negative parts) are observed. Here, we considered $N = 6$ emitters and no losses to other spatial modes. **(d)** Wigner function in mode 2.

IV.4 Dependance of fidelity on number of emitters

In this section, we investigate how the fidelity of state creation depends on the number of emitters involved. For simplicity, we consider emitters symmetrically coupled to a 1D waveguide. We investigate specifically the creation of a cat state $|\psi\rangle \propto |\alpha\rangle + |-\alpha\rangle$, with $\alpha = 2$. We initialize the emitters in a state for which elements in the Dicke basis match $|\psi\rangle$ in the Fock basis, truncating the state at the number of available emitters (while properly normalizing). In other words, given the density matrix $\rho^{\text{light}} = |\psi\rangle\langle\psi| = \sum_{0\leq i,j\leq\infty} \rho_{ij}^{\text{light}} |i\rangle\langle j|$, we initialize the emitters in a density

matrix $\rho^{\text{emitters}} \propto \sum_{0\le i,j\le N} \rho_{ij}^{\text{light}} |i\rangle\langle j|$. We then simulate the evolution and plot the fidelity of the emitted state in the dominant mode as a function of the number of emitters.

The results in Fig S7 show that the fidelity increases with the number of emitters. This occurs for two reasons: (I) For small numbers of emitters, truncation of the density matrix due to the finite number of emitters causes the state of light to differ from the cat state substantially. (II) For a smaller number of emitters, the initial state is more deeply in the nonlinear regime, causing the emission to populate multiple temporal modes and the first populated mode to decohere.

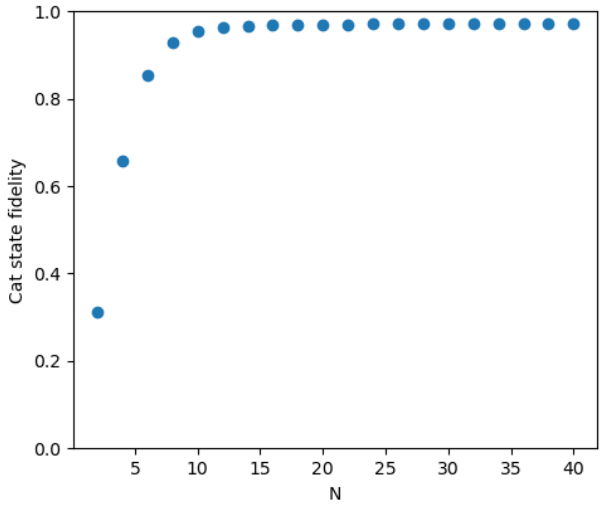

Fig. S7. Fidelity of Schrodinger cat state vs number of emitters. Showing the increase of fidelity with the number of emitters.

V Emitters in free space

In this section, we summarize how the theory can be applied to emitters in the three-dimensional free space. The emitters are at locations $\{\boldsymbol{x}_n\}$, with $n = 1,2,\dots,N$. The Hamiltonian of the system reads

$$H = H_{\text{E}} + H_{\text{F}} + H_{\text{EF}}, \tag{S46}$$

with

$$H_{\text{EF}} = \sum_{\mu} \int \frac{d^3\boldsymbol{k}}{(2\pi)^3} \sqrt{\frac{V\omega(\boldsymbol{k})\left(\boldsymbol{d}\cdot\boldsymbol{\varepsilon}_{\mu}\right)}{2\varepsilon_0}}\, a^{\dagger}(\boldsymbol{k})a(\boldsymbol{k}), \tag{S47}$$

$$H_{\text{E}} = \sum_{n} \sigma_n^z + H_{\text{I}}, \tag{S48}$$

$$H_{\text{F}} = \int d^3\boldsymbol{k}\omega(\boldsymbol{k})a^{\dagger}(\boldsymbol{k})a(\boldsymbol{k}), \tag{S49}$$

where H_{I} is a general interaction Hamiltonian between the emitters, for example for a dipole-dipole interaction it takes the form $H_{\mathrm{DD}} = \sum_{mn} J_{mn} \sigma_m^+ \sigma_n^-$ with J_{mn} defined by: $G(\boldsymbol{x}_m, \boldsymbol{x}_n, \Omega_0) = J_{mn} - \frac{i\Gamma_{mn}}{2}$ where $G(\boldsymbol{x}_m, \boldsymbol{x}_n, \omega)$ is the Greens function.

V.1 Input-output relation in three dimensions

The operator of vector field $\boldsymbol{A}^-(\boldsymbol{x}, t)$ is given by:

$$\boldsymbol{A}_\mu^-(\boldsymbol{x}, t) = \int_{-\infty}^{+\infty} d^3\boldsymbol{k} \frac{V}{(2\pi)^3} \sqrt{\frac{1}{2\varepsilon_0 \omega_{\boldsymbol{k}} V}}\, \boldsymbol{\varepsilon}_\mu a_\mu(\boldsymbol{k}, t) e^{i\boldsymbol{k}\boldsymbol{x}} \tag{S50}$$

We can define its Fourier transform by $\boldsymbol{A}^-(\boldsymbol{x}, \omega) = \frac{1}{\sqrt{2\pi}} \int \boldsymbol{A}^-(\boldsymbol{x}, t) e^{-i\omega t} dt$, and it obeys the equation [18]:

$$\nabla \times \nabla \times \boldsymbol{A}_\mu^-(\boldsymbol{x}, \omega) - \frac{\varepsilon(\boldsymbol{r})\omega^2}{c^2} \boldsymbol{A}_\mu^-(\boldsymbol{x}, \omega) = \frac{1}{\varepsilon_0 c^2} \boldsymbol{J}^-(\boldsymbol{x}, \omega). \tag{S51}$$

Its solution is given by:

$$\boldsymbol{A}_\mu^-(\boldsymbol{x}, \omega) = \boldsymbol{A}_{\mu 0}^-(\boldsymbol{x}, \omega) + \frac{1}{\varepsilon_0 c^2} \int \boldsymbol{G}(\boldsymbol{x}, \boldsymbol{x}', \omega) \boldsymbol{J}^-(\boldsymbol{x}, \omega) d^3\boldsymbol{x}'. \tag{S52}$$

Now $\boldsymbol{J}^-(\boldsymbol{x}, \omega) = \omega \boldsymbol{d} \sum_n \sigma_n^-(\omega) \delta(\boldsymbol{x} - \boldsymbol{x}_n)$ and $\boldsymbol{d}$ the dipole matrix element of the two-level transition. In free space, in the far field limit, Green's function is given by:

$$\boldsymbol{G}(\boldsymbol{x}, \boldsymbol{x_n}, \omega) \approx \frac{e^{\frac{i\omega}{c}|\boldsymbol{x} - \boldsymbol{x}_n|}}{4\pi x}. \tag{S53}$$

We can approximate $|\boldsymbol{x} - \boldsymbol{x}_n| \approx x - \hat{\boldsymbol{x}} \cdot \boldsymbol{x}_n$ leading to:

$$\boldsymbol{G}(\boldsymbol{x}, \boldsymbol{x_n}, \omega) \approx \frac{e^{\frac{i\omega}{c}(x - \hat{\boldsymbol{x}} \cdot \boldsymbol{x}_{\mathrm{n}})}}{4\pi x}. \tag{S54}$$

We get

$$A_\mu^-(\boldsymbol{x}, \omega) = A_{\mu 0}^-(\boldsymbol{x}, \omega) + \frac{\omega(\boldsymbol{d} \cdot \boldsymbol{\varepsilon}_\mu)}{4\pi x \varepsilon_0 c^2} \sum_n \sigma_n^-(\omega) \exp\left(\frac{i\omega}{c}(x - \hat{\boldsymbol{x}} \cdot \boldsymbol{x}_n)\right). \tag{S55}$$

We can now Fourier transform $(S55)$ to get:

$$A_\mu^-(\boldsymbol{x}, t) = A_{\mu 0}^-(\boldsymbol{x}, t) + \frac{\Omega_0(\boldsymbol{d} \cdot \boldsymbol{\varepsilon}_\mu)}{4\pi x \varepsilon_0 c^2} \sum_n \sigma_n^-\left(t - \frac{(x - \hat{\boldsymbol{x}} \cdot \boldsymbol{x}_n)}{c}\right). \tag{S56}$$

and finally make a Markov approximation assuming $\sigma_n^-\left(t - \frac{(x - \hat{\boldsymbol{x}} \cdot \boldsymbol{x}_n)}{c}\right) \approx \sigma_n^-\left(t - \frac{x}{c}\right) e^{-\frac{i\Omega_0 \hat{\boldsymbol{x}} \cdot \boldsymbol{x}_n}{c}}$ to get the desired result:

$$A_\mu^-(\boldsymbol{x},t) = A_{\mu 0}^-(\boldsymbol{x},t) + \frac{\Omega_0(\boldsymbol{d}\cdot\boldsymbol{\varepsilon}_\mu)}{4\pi x\varepsilon_0 c^2}\sum_n \sigma_n^-\left(t-\frac{x}{c}\right)e^{-\frac{i\Omega_0\hat{\boldsymbol{x}}\cdot\boldsymbol{x}_n}{c}}. \tag{S57}$$

Now we need to find $a_\mu(\boldsymbol{x},t) = \int_{-\infty}^{+\infty} a_\mu(\boldsymbol{k},t)e^{i\boldsymbol{k}\cdot\boldsymbol{x}}d^3\boldsymbol{k}$

$$A_\mu^-(\boldsymbol{x},t) = \int_{-\infty}^{+\infty} d^3\boldsymbol{k}\frac{V}{(2\pi)^3}\sqrt{\frac{1}{2\varepsilon_0\omega_{\boldsymbol{k}}V}}a_\mu(\boldsymbol{k},t)e^{i\boldsymbol{k}\boldsymbol{x}} \approx \frac{1}{(2\pi)^3}\sqrt{\frac{V}{2\varepsilon_0\Omega_0}}a_\mu(\boldsymbol{x},t). \tag{S58}$$

Thus, we get:

$$a_\mu(\boldsymbol{x},t) = a_{\mu 0}(\boldsymbol{x},t) + \frac{(\boldsymbol{d}\cdot\boldsymbol{\varepsilon}_\mu)}{x}\sqrt{\frac{8\pi^4\Omega_0^3}{V\varepsilon_0 c^4}}\sum_n \sigma_n^-\left(t-\frac{x}{c}\right)e^{-\frac{i\Omega_0\hat{\boldsymbol{x}}\cdot\boldsymbol{x}_n}{c}}. \tag{S59}$$

We define

$$S^-(\theta,\phi,t-x/c) \equiv \sum_n \sigma_n^-\left(t-\frac{x}{c}\right)e^{-\frac{i\Omega_0\hat{\boldsymbol{x}}\cdot\boldsymbol{x}_n}{c}}, \qquad \kappa = \sqrt{\frac{8\pi^4\Omega_0^3}{V\varepsilon_0 c^4}}. \tag{S60}$$

We get input-output relation:

$$a_\mu(\boldsymbol{x},t) = a_{\mu 0}(\boldsymbol{x},t) + \frac{(\boldsymbol{d}\cdot\boldsymbol{\varepsilon}_\mu)}{x}\kappa S^-(\theta,\phi,t-x/c). \tag{S61}$$

V.2 Spatiotemporal modes

The modes can be found from $\Gamma^{(1)}$ matrix, similar to the 1D case:

$$\Gamma_\mu^{(1)}(\theta_1,\phi_1,t_1;\theta_2,\phi_2,t_2) = \left\langle a_\mu^\dagger(\boldsymbol{x}_1,t_1)a_\mu(\boldsymbol{x}_2,t_2)\right\rangle =$$
$$= \frac{\left|\boldsymbol{d}\cdot\boldsymbol{\varepsilon}_\mu\right|^2}{x^2}|\kappa|^2\left\langle S^+\left(\theta_1,\phi_1,t_1-\frac{x_1}{c}\right)S^-\left(\theta_2,\phi_2,t_2-\frac{x_2}{c}\right)\right\rangle. \tag{S62}$$

The matrix $\Gamma^{(1)}$ can be diagonalize to find the principal modes:

$$\Gamma_\mu^{(1)}(\theta_1,\phi_1,t_1;\theta_2,\phi_2,t_2) = \sum_i n_{\mu i}\eta_{\mu i}^*(\theta_1,\phi_1,t_1)\eta_{\mu i}(\theta_2,\phi_2,t_2) \tag{S63}$$

Then the mode is defined as:

$$a_{\mu i} = \int dt\int d\Omega\,\eta_{\mu i}^*(\theta,\phi,t)a_{\mu i}(\theta,\phi,t) \tag{S64}$$

where $a_{\mu i}(\theta,\phi,t) \equiv a_{\mu i}(\boldsymbol{x},t) \equiv a_{\mu i}(\theta,\phi,t-x/c)$.

The modes a_i should obey standard commutation relations $\left[a_i,a_j^\dagger\right] = \delta_{i,j}$. From this requirement we get additional condition on $\eta_{\mu i}^*(\theta,\phi,t)$ to be normalized and orthogonal:

$$\int dt\int d\Omega\,\eta_{\mu i}^*(\theta,\phi,t)\eta_{\mu' j}(\theta,\phi,t) = \delta_{i,j}\delta_{\mu\mu'} \tag{S65}$$

V.3 Master equation for the evolution of the emitter system and the considered mode

Similar to the 1D case, we can get the master equation that will describe the evolution of a_0. For this we first start from the equation for the emitters. The evolution of the emitters in free space including dissipative and coherent interactions is given by the following Master equation [19]:

$$\dot{\rho}_{\mathrm{E}} = -i[H_{\mathrm{E}}, \rho_{\mathrm{E}}] + \sum_{m,n} \frac{\Gamma_{mn}}{2} (2\sigma_m^- \rho_{\mathrm{E}} \sigma_n^+ - \{\sigma_n^+ \sigma_m^-, \rho_{\mathrm{E}}\}) , \tag{S66}$$

with $\rho_{\mathrm{E}} = \mathrm{Tr}_{\mathrm{light}}(\rho(t))$. We diagonalize the second part of Eq (S49) and get:

$$\dot{\rho}_{\mathrm{E}} = -i[H_{\mathrm{E}}, \rho_{\mathrm{E}}] + \sum_{\nu} \frac{\Gamma_\nu}{2} (2O_\nu^- \rho_{\mathrm{E}} O_\nu^+ - \{O_\nu^+ O_\nu^-, \rho_{\mathrm{E}}\}) . \tag{S67}$$

where $O_\nu^- = \sum_n U_{\nu n}^\dagger \sigma_n^-$ with U being the unitary matrix that diagonalizes Γ. Using the input-output relation, we can write the differential equation for a_0:

$$\dot{a}_0 = \int d\Omega\, \eta_{\mu 0}^*(\theta, \phi, t) \frac{(\boldsymbol{d} \cdot \boldsymbol{\varepsilon}_\mu)}{x} \kappa \sum_n \sigma_n^- \left(t - \frac{x}{c}\right) e^{-\frac{i\Omega_0 \hat{\boldsymbol{x}} \cdot \boldsymbol{x}_n}{c}} . \tag{S68}$$

Since $\sigma_n = \sum_n U_{n\nu} O_\nu^-$, we get:

$$\dot{a}_0 = \sum_\nu O_\nu^-(t - x/c) \int d\Omega\, \eta_{\mu 0}^*(\theta, \phi, t) \frac{(\boldsymbol{d} \cdot \boldsymbol{\varepsilon}_\mu)}{x} \kappa \sum_n U_{n\nu} e^{-\frac{i\Omega_0 \hat{\boldsymbol{x}} \cdot \boldsymbol{x}_n}{c}} . \tag{S69}$$

We define coefficient $\zeta_\nu(t)$ such that

$$\zeta_\nu(t) \equiv 1/\sqrt{\Gamma_\nu} \int d\Omega\, \eta_\mu^*(\theta, \phi, t) \frac{(\boldsymbol{d} \cdot \boldsymbol{\varepsilon}_\mu)}{x} \kappa \sum_n U_{n\nu} e^{-\frac{i\Omega_0 \hat{\boldsymbol{x}} \cdot \boldsymbol{x}_n}{c}} . \tag{S70}$$

According to this definition, we get:

$$\dot{a}_0 = \sum_\nu \sqrt{\Gamma_\nu} \zeta_\nu(t) O_\nu^-(t - x/c) . \tag{S71}$$

Similar to the 1D case, we arrive to the following master equation for mode a_η:

$$\dot{\rho} = -i[H_{\mathrm{S}} + H_{\mathrm{I}}, \rho] + \sum_\nu \frac{1}{2} (2L_\nu^- \rho L_\nu^+ - \{L_\nu^+ L_\nu^-, \rho\}) , \tag{S72}$$

where $H_{\mathrm{I}} = \frac{i}{2} \sum_\nu \sqrt{\Gamma_\nu} (\zeta_\nu^*(t) O_\nu^+ a_0 - \zeta_\nu(t) O_\nu^- a_0^\dagger)$ and $L_\nu(t) = \sqrt{\Gamma_\nu} O_\nu^- + \zeta_\nu^*(t) a_0$. The final term in (S72) is meant to cancel the terms that create an excitation in the system and remove a photon from the virtual cavity.

$$-i[H_S,\rho]+\frac{1}{2}\sum_\nu\sqrt{\Gamma_\nu}\left[\zeta_\nu^*(t)a_0O_\nu^+-\zeta_\nu(t)a_0^\dagger O_\nu^-,\rho\right]+\sum_\nu\left(L_\nu\rho L_\nu^\dagger-\frac{1}{2}\{L_\nu^\dagger L_\nu,\rho\}\right)=$$
$$-i[H_S,\rho]+\frac{1}{2}\sum_\nu\sqrt{\Gamma_\nu}\left[\zeta_\nu(t)a_0^\dagger O_\nu^--\zeta_\nu^*(t)a_0O_\nu^+,\rho\right]$$
$$+\sum_\nu\left(\sqrt{\Gamma_\nu}O_\nu^-+\zeta_\nu^*(t)a_0\right)\rho\left(\sqrt{\Gamma_\nu}O_\nu^++\zeta_\nu(t)a_0^\dagger\right)$$
$$-\frac{1}{2}\{\left(\sqrt{\Gamma_\nu}O_\nu^++\zeta_\nu(t)a_0^\dagger\right)\left(\sqrt{\Gamma_\nu}O_\nu^-+\zeta_\nu^*(t)a_0\right),\rho\}) \tag{S73}$$

Opening the brackets gives:

$$\dot\rho=-i[H_S,\rho]+\frac{1}{2}\sum_\nu\sqrt{\Gamma_\nu}\left(\zeta_\nu^*(t)a_0O_\nu^+\rho-\zeta_\nu(t)a_0^\dagger O_\nu^-\rho+\zeta_\nu(t)\rho a_0^\dagger O_\nu^--\zeta_\nu^*(t)\rho a_0O_\nu^+\right)$$
$$+\left(\Gamma_\nu O_\nu^-\rho O_\nu^++\sqrt{\Gamma_\nu}\zeta_\nu^*(t)a_0\rho O_\nu^++\sqrt{\Gamma_\nu}\zeta_\nu(t)O_\nu^-\rho a_0^\dagger+|\zeta_\nu(t)|^2a_0\rho a_0^\dagger\right)$$
$$-\frac{1}{2}(\Gamma_\nu O_\nu^+O_\nu^-\rho+\sqrt{\Gamma_\nu}\zeta_\nu^*(t)O_\nu^+a_0\rho+|\zeta_\nu(t)|^2a_0^\dagger a_0\rho+\sqrt{\Gamma_\nu}\zeta_\nu(t)O_\nu^-a_0^\dagger\rho+\Gamma_\nu O_\nu^+O_\nu^-\rho$$
$$+\sqrt{\Gamma_\nu}\zeta_\nu^*(t)\rho O_\nu^+a_0+|\zeta_\nu(t)|^2\rho a_0^\dagger a_0+\sqrt{\Gamma_\nu}\zeta_\nu(t)\rho O_\nu^-a_0^\dagger) \tag{S74}$$

Now notice the cancelation of the first and third terms in the interaction Hamiltonian, with the damping terms:

$$\dot\rho=-i[H_S,\rho]+\sum_\nu\sqrt{\Gamma_\nu}\left(-\zeta_\nu(t)a_0^\dagger O_\nu^-\rho-\zeta_\nu^*(t)\rho a_0O_\nu^+\right)$$
$$+\left(\sqrt{\Gamma_\nu}\zeta_\nu^*(t)\rho O_\nu^+a_0+\sqrt{\Gamma_\nu}\zeta_\nu^*(t)a_0\rho O_\nu^++\sqrt{\Gamma_\nu}\zeta_\nu(t)O_\nu^-\rho a_0^\dagger+\sqrt{\Gamma_\nu}\zeta_\nu(t)O_\nu^-a_0^\dagger\rho\right)$$
$$+\Gamma_\nu\left(O_\nu^-\rho O_\nu^+-\frac{1}{2}\{O_\nu^+O_\nu^-,\rho\}\right)+|\zeta_\nu(t)|^2\left(a_0\rho a_0^\dagger-\frac{1}{2}\{a_0^\dagger a_0,\rho\}\right) \tag{S75}$$

Which exactly gives the dissipators for the cavity and the system, along with the single direction couplings from the system to the virtual cavity.

VI. Initial Atomic state

In this section, we will provide the explicit forms of the density matrices for the initial conditions considered in the main text and discuss ideas to obtain them experimentally. In Figure 2, 3a, and 4a, we consider a fully excited initial condition $|N\rangle$. This is a standard initial condition and can be obtained via a coherent excitation π-pulse. In Figures 3c, and 4 and 5b, the initial state is an atomic cat state, given by

$$|\psi_{2\text{cat}}\rangle\propto(\exp(iS_x\theta)+\exp(-iS_x\theta))|0\rangle\,, \tag{S76}$$

with $\theta = 1.3$ in Figure 3c and $\theta = \pi/2$ in Figure 4b and 5. Experimentally, such a state can be realized following a protocol recently proposed with a nonlinear Stark shift [20], with an ensemble of three-level emitters in detuned cavity, using a light source with a detuned frequency. Another way to create such states is by intense squeezing, for example with bicolor excitations that allow for specific double-Raman transitions. Examples of such state preparation are presented in ref [21]–[23]. In the intense squeezing case, we take advantage of the relation:

$$\exp(iS_x^2\pi/2)\exp(iS_x\theta_2)\,|0\rangle \propto \left(\exp(iS_x\theta_2) - i\exp\left(iS_x(\pi-\theta_2)\right)\right)|0\rangle, \tag{S77}$$

with $\theta_2 = 1.3$. The operators $\exp(iS_x\theta_2)$ can be implemented by coherent laser excitations, whereas $\exp(iS_x^2\pi/2)$ can arise in the case of multicolor excitations [21]. Next, in Figure 3b we consider atomic GKP states, namely:

$$|\psi_{\mathrm{GKP}}\rangle \propto \left(D(\alpha) + D(-\alpha)\right)^N S(r)|0\rangle, \tag{S78}$$

where $D(\alpha)$ is the photonic displacement operator and $S(r)$ the photonic squeezing operator. We then truncate the coefficients of the density matrix at the number of emitters and normalize the state. We use $\alpha = \sqrt{\pi/2}$ and $r = 0.5\ln(2)$ for 10dB squeezing and $N = 40$ emitters. The last state we consider as an initial condition for the emitters is a squeezed state:

$$\left|\psi_{\mathrm{squeezed}}\right\rangle = \exp(iS_x^2\theta_4)|0\rangle\,, \tag{S79}$$

with $\theta_4 = 0.3$.

[1] M. Tavis and F. W. Cummings, "Exact Solution for an N-Molecule---Radiation-Field Hamiltonian," *Physical Review*, vol. 170, no. 2, pp. 379–384, Jun. 1968, doi: 10.1103/PhysRev.170.379.

[2] M. TAVIS and F. W. CUMMINGS, "Approximate Solutions for an N-Molecule-Radiation-Field Hamiltonian," *Physical Review*, vol. 188, no. 2, pp. 692–695, Dec. 1969, doi: 10.1103/PhysRev.188.692.

[3] R. Bonifacio, P. Schwendimann, and F. Haake, "Quantum statistical theory of superradiance. II," *Phys Rev A (Coll Park)*, vol. 4, no. 3, p. 854, 1971.

[4] R. Bonifacio, P. Schwendimann, and F. Haake, "Quantum statistical theory of superradiance. I," *Phys Rev A (Coll Park)*, vol. 4, no. 1, p. 302, 1971.

[5] J. P. Dowling, G. S. Agarwal, and W. P. Schleich, "Wigner distribution of a general angular-momentum state: Applications to a collection of two-level atoms," *Phys Rev A (Coll Park)*, vol. 49, no. 5, p. 4101, 1994.

[6] E. P. Wigner, "On the quantum correction for thermodynamic equilibrium," *Part I: Physical Chemistry. Part II: Solid State Physics*, pp. 110–120, 1997.

[7] C. Gerry, P. Knight, and P. L. Knight, *Introductory quantum optics*. Cambridge university press, 2005.

[8] J. Eisert, M. Cramer, and M. B. Plenio, "Colloquium: Area laws for the entanglement entropy," *Rev Mod Phys*, vol. 82, no. 1, pp. 277–306, Feb. 2010, doi: 10.1103/RevModPhys.82.277.

[9] K. Życzkowski, P. Horodecki, A. Sanpera, and M. Lewenstein, “Volume of the set of separable states,” *Phys Rev A (Coll Park)*, vol. 58, no. 2, pp. 883–892, Aug. 1998, doi: 10.1103/PhysRevA.58.883.
[10] C. Fabre and N. Treps, “Modes and states in quantum optics,” *Rev Mod Phys*, vol. 92, no. 3, p. 35005, Sep. 2020, doi: 10.1103/RevModPhys.92.035005.
[11] A. H. Kiilerich and K. Mølmer, “Input-output theory with quantum pulses,” *Phys Rev Lett*, vol. 123, no. 12, p. 123604, 2019.
[12] A. H. Kiilerich and K. Mølmer, “Quantum interactions with pulses of radiation,” *Phys Rev A (Coll Park)*, vol. 102, no. 2, p. 23717, Aug. 2020, doi: 10.1103/PhysRevA.102.023717.
[13] M. O. Scully and M. S. Zubairy, “Quantum optics.” American Association of Physics Teachers, 1999.
[14] C. W. Gardiner and M. J. Collett, “Input and output in damped quantum systems: Quantum stochastic differential equations and the master equation,” *Phys Rev A (Coll Park)*, vol. 31, no. 6, p. 3761, 1985.
[15] M. Lax, “Quantum noise. X. Density-matrix treatment of field and population-difference fluctuations,” *Physical Review*, vol. 157, no. 2, p. 213, 1967.
[16] C. Gardiner, P. Zoller, and P. Zoller, *Quantum noise: a handbook of Markovian and non-Markovian quantum stochastic methods with applications to quantum optics*. Springer Science & Business Media, 2004.
[17] T. Caneva, M. T. Manzoni, T. Shi, J. S. Douglas, J. I. Cirac, and D. E. Chang, “Quantum dynamics of propagating photons with strong interactions: a generalized input–output formalism,” *New J Phys*, vol. 17, no. 11, p. 113001, 2015, doi: 10.1088/1367-2630/17/11/113001.
[18] L. Novotny and B. Hecht, *Principles of Nano-Optics*, 2nd ed. Cambridge: Cambridge University Press, 2012. doi: DOI: 10.1017/CBO9780511794193.
[19] A. Asenjo-Garcia, M. Moreno-Cardoner, A. Albrecht, H. J. Kimble, and D. E. Chang, “Exponential Improvement in Photon Storage Fidelities Using Subradiance and ``Selective Radiance'' in Atomic Arrays,” *Phys Rev X*, vol. 7, no. 3, p. 31024, Aug. 2017, doi: 10.1103/PhysRevX.7.031024.
[20] Y. Zhao, R. Zhang, W. Chen, X.-B. Wang, and J. Hu, “Creation of Greenberger-Horne-Zeilinger states with thousands of atoms by entanglement amplification,” *npj Quantum Inf*, vol. 7, no. 1, p. 24, 2021.
[21] A. S. Sørensen and K. Mølmer, “Entangling atoms in bad cavities,” *Phys Rev A (Coll Park)*, vol. 66, no. 2, p. 022314, 2002.
[22] G. S. Agarwal, R. R. Puri, and R. P. Singh, “Atomic Schr\"odinger cat states,” *Phys Rev A (Coll Park)*, vol. 56, no. 3, pp. 2249–2254, Sep. 1997, doi: 10.1103/PhysRevA.56.2249.
[23] K. Mølmer and A. Sørensen, “Multiparticle entanglement of hot trapped ions,” *Phys Rev Lett*, vol. 82, no. 9, p. 1835, 1999.